Ballistic transport in quantum channels modulated with double-bend structures

Hongqi Xu*
Department of Physics and Measurement Technology, Linköping University, S-581 83 Linköping, Sweden and Department of Solid State Physics, University of Lund, Box 118, S-221 00 Lund, Sweden
(Received 28 May 1992; revised manuscript received 21 September 1992)

We report on quantum-mechanical calculations of ballistic transport in finite quantum channels with single and multiple double-bend discontinuities. The channels connect to two semi-infinite two-dimensional electron gases, which serve as emitter and collector when a potential difference is applied. The calculations are performed by use of a transfer-matrix method formulated by using one common basis for all matrices required for the description of the electron states in the finite channel. It is shown that in the quantum channel with a single double-bend discontinuity, at least one conductance peak can be found at an energy below the threshold of the first plateau. These peaks appear due to resonant tunneling via quasibound states at energies below the first transverse mode. It is also shown that in the quantum channel with a multiple double-bend discontinuity the quasibound states in different double-bend regions couple to each other, leading to multiple splits of the conductance peaks. Critical discussions on recent experimental measurements and theoretical calculations on electron transport in doubly bent quantum channels are presented. We emphasize the fact that the quasibound states can be probed by electron transmissions only if the doubly bent channel is of finite length, and only if we also consider the electron states in much wider outside regions connected with the channel.

I. INTRODUCTION

Recent advances in nanostructure technology[1] have made it possible to define constrictions, with lateral dimensions of 100 nm or less, in a two-dimensional electron gas (2DEG) formed at a semiconductor heterostructure, resulting in the fabrication of quantum wires, constrictions, and quantum dots. In such a small structure, electron transport is ballistic and the motion of electrons is governed by quantum mechanics rather than classical mechanics, revealing a few interesting features in electron transport.[2] The quantization of the conductance of narrow constrictions observed by van Wees *et al.*[3] and Wharam *et al.*[4] and the resonant conductance via quasibound states in classically unbound systems[5,6] are just two examples of recent developments in this area.

Based on the one-electron Schrödinger equation, Kirczenow[7] has performed calculations for the electron conductance of narrow ballistic constrictions in a 2DEG and the quantization of conductance in units of $2e^2/h$ has been obtained. In addition, the calculations have predicted that in such a quantum channel, the conductance should oscillate strongly as a function of the Fermi energy, due to the presence of longitudinal resonant states. Schult, Ravenhall, and Wyld[8] have calculated the energies and wave functions for an electron in the intersecting narrow channels of infinite length and have found quantum bound states. When the channels are sufficiently short and are connected to the two-dimensional electron reservoirs, the quantum bound states will couple to the continuous state of the 2DEG's, leading to the formation of quasibound or resonant states. The quantum-mechanical calculations by Berggren and Ji[6] for the electron transport in the intersecting channels of finite length have convincingly associated the sharp resonances in the conductance to the quasibound states in such ballistic systems. Electron transport in ballistic lateral superlattices consisting of finite periods of intersections[9] or *T*-shaped structures[10,11] has also been studied theoretically. In these calculations, conductance gaps and strong oscillations have been found, indicating the formation of electron miniband structures in these superlattices. The experimental observation of the gaps and the oscillations in the conductance of a *T*-shaped superlattice has been reported.[5]

An experimental investigation on electron transport in a finite and doubly bent quantum channel was recently performed by Wu *et al.*[12] Fine resonant peaks superimposed on the conductance plateaus of the quantum system were observed and were assumed to be due to quantum interference in the double-bend region. In addition, Wu *et al.* observed also two sharp peaks in the conductance of the doubly bent quantum channel below the threshold of the lowest plateau. They associated these two peaks with resonant tunneling through impurity states in the channel.[12] On the other hand, theoretical calculations by Exner and Seba,[13] Sols and Macucci,[14] Avishai *et al.*,[15] and Goldstone and Jaffe[16] have predicted that in a singly bent quantum channel of infinite length there can exist at least one bound state below the first transverse-mode energy. When the channel is of finite length, the bound state can be coupled to the continuous states in the outside of the channel and becomes quasibound. Thus resonant tunneling via the quasibound state can occur. This will give rise to a resonant peak in conductance below the threshold of the lowest conductance plateau. From this analysis, one can expect that quasibound states with energies below the first transverse-mode energy should exist in the doubly bent quantum channel studied experimentally by Wu *et al.* As a consequence, one may expect to observe conductance peaks corresponding to resonant tunneling via these quasibound states in this quantum system. However, recent theoretical calculations by Weisshaar *et al.*[17]

 ©1993 The American Physical Society

on transmission probabilities of a quantum channel with a double bend and of infinite length give no indication of the appearance of such resonant peaks in conductance and no indication of the existence of bound or quasibound states below the first transverse-mode energy either. This does not mean that there calculations are in disagreement with the calculations by Exner and Seba, Sols and Macucci, Avishai *et al.*, and Goldstone and Jaffe, but rather indicates that it is essential to make channels be of finite length in order to probe bound states (or precisely quasibound states in these cases) by means of electron transmission.

In this paper, we report on quantum-mechanical calculations for ballistic electron transport in short quantum channels consisting of a finite number of double bends and being connected with the two semi-infinite 2DEG's. We will idealize the systems by assuming that the geometries of the multiply bent channels are formed by embedding rectangular barriers of finite height in a narrow straight channel delimited by hard-wall boundaries. When the height is sufficiently large, our single double-bend structure will be in analogy to the channel structure studied experimentally in Ref. 12. We will show that the conductance peaks corresponding to resonant tunneling via quasibound states below the first transverse-mode energy should appear in a quantum channel of a constant width and with a double right-angle bend (or, simply, a double bend). Our calculations are done with the use of transfer-matrix method formulated by basing all our matrices throughout the quantum channels on one common basis. The method has a great flexibility, i.e., it can be easily used to treat electron transport in the quantum channels having very complicated structures in both the longitudinal and the transverse directions.

The rest of the paper is organized as follows. In Sec. II we describe the method of calculations. In Sec. III we present and analyze the calculated results for the conductance of the ballistic channels with a double bend. Our calculated results for the channels with multiple double bends are also presented and discussed in this section. Section IV contains a summary and some concluding remarks.

II. THEORETICAL METHOD

We consider a quantum ballistic channel having electrons confined by the hard-wall boundaries along the y direction but allowed to move along the x direction. We further assume that the channel can be divided along the longitudinal x direction into strips which are small enough so that the potential in each strip is of transverse y-direction dependence only. This is illustrated in Fig. 1 where the quantum channel has been partitioned into N strips. The Schrödinger equation of motion of an electron with energy ε in strip region i in the channel can then be written as

$$\left[-\frac{\hbar^2}{2m^*}\left[\frac{\partial^2}{\partial x^2}+\frac{\partial^2}{\partial y^2}\right]+V_c(y)+V_b^i(y)\right]\Psi^i(x,y) = \varepsilon\Psi^i(x,y) , \quad (1)$$

where m^* is the effective mass, the confinement potential $V_c(y)$ is zero inside the entire channel and infinite outside, and $V_b^i(y)$ describes the electron potential in the strip region i. In the considered strip region, the wave function that satisfies Eq. (1) can be written as

$$\Psi^i(x,y)=\sum_\alpha [b_\alpha^i e^{ik_\alpha^i(x-x_0^i)}+c_{\alpha^i} e^{-ik_\alpha^i(x-x_0^i)}]\varphi_\alpha^i(y) , \quad (2)$$

where x_0^i is the reference coordinate along the x direction for the strip region i and has been specified in Fig. 1, and $\varphi_\alpha^i(y)$ are a set of transverse eigenstates in this strip region with eigenvalues E_α^i. The quantities k_α^i can be expressed in terms of E_α^i and the energy ε of the electrons injected into the region,

$$k_\alpha^i=\left[\frac{2m^*(\varepsilon-E_\alpha^i)}{\hbar^2}\right]^{1/2} . \quad (3)$$

For a fixed ε, k_α^i can be either real or imaginary. In the case that k_α^i is imaginary, the convention $(-1)^{1/2}=i$ will be used. We must sum over all α values in Eq. (2) to include all evanescent and current transporting waves as demanded by completeness.

If the potential $V_b^i(y)$ is zero everywhere in the quantum channel, the confinement potential $V_c(y)$ should give rise to a set of normal modes $\Phi_n(y)$ which satisfy the one-dimensional Schrödinger equation

$$\left[-\frac{\hbar^2}{2m^*}\frac{d^2}{dy^2}+V_c(y)\right]\Phi_n(y)=\varepsilon_n\Phi_n(y) , \quad (4)$$

where n is the index of the normal modes and ε_n are the normal mode energies. We will use this set of normal modes $\Phi_n(y)$ as our basis throughout the channel. By projecting the transverse eigenstates $\varphi_\alpha^i(y)$ onto this basis,

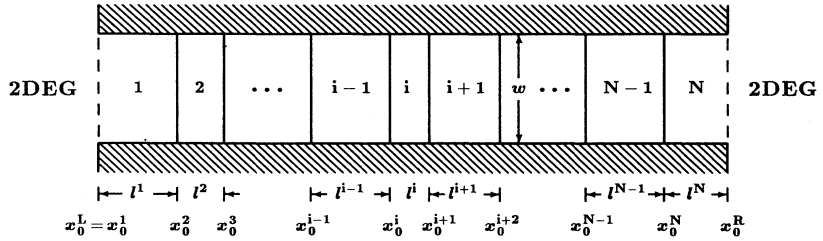

FIG. 1. Schematic diagram of a finite quantum channel in which the electron potential varies along both the transportation x and the transverse y directions. The channel is connected with two semi-infinite 2DEG's and has been partitioned into N strip regions in such a way that in each strip region the electron potential only varies along the transverse y direction.

Eq. (2) can be rewritten as

$$\Psi^i(x,y)=\sum_n \Phi_n(y)\sum_\alpha d^i_{n\alpha}[b^i_\alpha e^{ik^i_\alpha(x-x^i_0)} + c^i_\alpha e^{-ik^i_\alpha(x-x^i_0)}] , \quad (5)$$

where the expansion coefficients $d^i_{n\alpha}$ for the strip region i are obtained by searching for their corresponding eigenvalues E^i_α from the system

$$\sum_m \{(\varepsilon_n - E^i_\alpha)\delta_{nm} + \langle \Phi_n(y)|V^i_b(y)|\Phi_m(y)\rangle\} d^i_{m\alpha}=0 , \quad n=1,2,3\ldots . \quad (6)$$

Once Eq. (6) is solved, the coefficients b^i_α and c^i_α in Eq. (5) are the remaining unknowns in the expansion for the wave function $\Psi^i(x,y)$ in the considered strip region i. Obviously, we have a set of coefficients b^i_α and c^i_α for each strip region. However, the connection between the coefficients of any two strip regions in the channel can be achieved by a transfer-matrix method.

Let us consider two adjacent regions i and $i+1$ as shown in Fig. 1. Using the usual wave-function-matching conditions, we can express the coefficients b^i_α and c^i_α appearing in the expansion for the wave function $\Psi^i(x,y)$ in the region i in terms of the coefficients b^{i+1}_α and c^{i+1}_α appearing in the expansion for the wave function $\Psi^{i+1}(x,y)$ in the region $i+1$. The result may be written in a matrix form as

$$\begin{bmatrix}\mathbf{B}^i\\ \mathbf{C}^i\end{bmatrix} = M(i,i+1)\begin{bmatrix}\mathbf{B}^{i+1}\\ \mathbf{C}^{i+1}\end{bmatrix} , \quad (7)$$

where $\mathbf{B}^i$ and $\mathbf{C}^i$ are coefficient vectors, whose elements are $\{b^i_\alpha\}$ and $\{c^i_\alpha\}$, respectively, and $M(i,i+1)$ is the transfer matrix which relates the coefficient vectors $\mathbf{B}^i$ and $\mathbf{C}^i$ to the coefficient vectors $\mathbf{B}^{i+1}$ and $\mathbf{C}^{i+1}$. It can be shown that the transfer matrix $M(i,i+1)$ is

$$M(i,i+1)=\begin{bmatrix}\gamma^i & 0\\ 0 & (\gamma^i)^{-1}\end{bmatrix}^{-1}\begin{bmatrix}P^i & P^i\\ Q^i & -Q^i\end{bmatrix}^{-1} \times \begin{bmatrix}P^{i+1} & P^{i+1}\\ Q^{i+1} & -Q^{i+1}\end{bmatrix} , \quad (8)$$

where γ^i is the diagonal matrix with elements given by $(\gamma^i)_{\alpha\alpha}=\exp(ik^i_\alpha l^i)$ and the submatrices P^i and Q^i are defined by $(P^i)_{n\alpha}=d^i_{n\alpha}$ and $(Q^i)_{n\alpha}=d^i_{n\alpha}k^i_\alpha w$. Here l^i is the width of the ith strip region along the x direction and w is the width of the straight square-well channel (see Fig. 1). It can be seen that all elements of the matrices are dimensionless. If the channel is divided into N strips as we have shown in Fig. 1, it is straightforward to show that the connection between the coefficient vectors at the two end strip region is

$$\begin{bmatrix}\mathbf{B}^1\\ \mathbf{C}^1\end{bmatrix} = M(1,N)\begin{bmatrix}\mathbf{B}^N\\ \mathbf{C}^N\end{bmatrix} , \quad (9)$$

where the transfer matrix $M(1,N)$ is given by

$$M(1,N) = M(1,2)M(2,3)\cdots M(N-2,N-1)M(N-1,N) . \quad (10)$$

By inversing $M(1,N)$, one can also express the coefficient vectors $\mathbf{B}^N$ and $\mathbf{C}^N$ in terms of the coefficient vectors $\mathbf{B}^1$ and $\mathbf{C}^1$. We note that, beside the structure parameters of the quantum channel, the transfer matrix $M(1,N)$ is energy-dependent only [see Eqs. (3) and (8)].

Now, we discuss the boundary conditions imposed on the wave function at the two ends of the quantum channel. One type of commonly used boundary conditions is to connect the finite quantum channel with two perfect infinitely long leads. Here we prefer to use another type of commonly used boundary conditions, that is, we connect the quantum channel to the 2DEG's as shown in Fig. 1. We are doing so not only because this boundary condition is more realistic to the device structures studied in many experiments, but also because it is crucial in order to probe localized electron states by means of electron transmission.

Consider an electron with wave vector $\mathbf{k}=(k_x,k_y)$ and energy ε, where $\varepsilon=\hbar^2(k_x^2+k_y^2)/(2m^*)$, incident on the channel from the left 2DEG reservoir. For $x<x^L_0\equiv x^1_0$, its wave function can be written as

$$\Psi^L(x,y)=e^{ik_x(x-x^L_0)}\phi^{2D}_{k_y}(y) + \int_{-\infty}^{\infty} dk'_y A^L_{k'_y} e^{-ik'_x(x-x^L_0)}\phi^{2D}_{k'_y}(y) , \quad (11)$$

where $\phi^{2D}_{k_y}(y)=(2\pi)^{-1/2}\exp(ik_y y)$, $k'_x=[2m^*\varepsilon/\hbar^2-(k'_y)^2]^{1/2}$. Here, the integral is taken over all transverse components k'_y and thus k'_x can be either real or imaginary, i.e., evanescent waves are again included. For the electron emitted from the channel in $x>x^R_0$, the wave function is

$$\Psi^R(x,y)=\int_{-\infty}^{\infty} dk'_y A^R_{k'_y} e^{ik'_x(x-x^R_0)}\phi^{2D}_{k'_y}(y) . \quad (12)$$

As usual, $\Psi^L(x,y)$ needs to be matched to $\Psi^1(x,y)$ at $x=x^L_0$ and $\Psi^R(x,y)$ to $\Psi^N(x,y)$ at $x=x^R_0$ with the requirement that amplitudes and derivatives with respect to x are equal. After eliminating $A^L_{k'_y}$, we can derive the boundary condition imposed on the coefficient vectors $\mathbf{B}^1$ and $\mathbf{C}^1$ in a matrix form as

$$S(1)\begin{bmatrix}\mathbf{B}^1\\ \mathbf{C}^1\end{bmatrix} \equiv \begin{bmatrix}T^1_+ & T^1_-\\ \mathbf{0} & \mathbf{0}\end{bmatrix}\begin{bmatrix}\mathbf{B}^1\\ \mathbf{C}^1\end{bmatrix} = \begin{bmatrix}\Lambda\\ \mathbf{0}\end{bmatrix} , \quad (13)$$

where, with w again as the width of the straight square-well channel, the vector Λ is defined by

$$(\Lambda)_n = 2k_x w\lambda_{nk_y} , \quad (14)$$

with

$$\lambda_{nk_y}=\int_{-\infty}^{\infty} dy\, \Phi^*_n(y)\phi^{2D}_{k_y}(y) , \quad (15)$$

and the submatrices T^i_+ and T^i_- (here $i=1$) are defined by

$$(T_{\pm}^{i})_{n\alpha}=\sum_{m}(t_{nm}d_{m\alpha}^{i}\pm\delta_{nm}d_{m\alpha}^{i}k_{\alpha}^{i})w \ , \tag{16}$$

with

$$t_{nm}=\int_{-\infty}^{\infty}dk_{y}'k_{x}'\lambda_{nk_{y}'}\lambda_{k_{y}'n} \ . \tag{17}$$

Similarly, after eliminating $A_{k_y'}^{R}$, we can derive the boundary condition imposed on the coefficient vectors $\mathbf{B}^N$ and $\mathbf{C}^N$ as

$$S(N)\begin{bmatrix}\gamma^{N} & 0\\ 0 & (\gamma^{N})^{-1}\end{bmatrix}\begin{bmatrix}\mathbf{B}^{N}\\ \mathbf{C}^{N}\end{bmatrix}=0 \ , \tag{18}$$

where

$$S(N)\equiv\begin{bmatrix}0 & 0\\ T_{-}^{N} & T_{+}^{N}\end{bmatrix} . \tag{19}$$

We note that for a given channel structure, the matrices $S(1)$ and $S(N)$ are energy dependent only, while the vector $\mathbf{\Lambda}$ depends on both the energy ε and the direction of the wave vector $\mathbf{k}$ of the electron in the 2DEG incident on the channel. Using Eqs. (13) and (18), the coefficient vectors $\mathbf{B}^1$ and $\mathbf{C}^1$ or the coefficient vectors $\mathbf{B}^N$ and $\mathbf{C}^N$ may be eliminated from Eq. (9) and thus the system equation for the expansion coefficients of the wave function in either one of the two end strip regions may be obtained. For example, by eliminating $\mathbf{B}^N$ and $\mathbf{C}^N$, we obtain

$$[S(1)+S(N)\Gamma(N)M^{-1}(1,N)]\begin{bmatrix}\mathbf{B}^{1}\\ \mathbf{C}^{1}\end{bmatrix}=\begin{bmatrix}\mathbf{\Lambda}\\ 0\end{bmatrix} , \tag{20}$$

where $\Gamma(N)$ is

$$\Gamma(N)=\begin{bmatrix}\gamma^{N} & 0\\ 0 & (\gamma^{N})^{-1}\end{bmatrix} . \tag{21}$$

Thus the coefficient vectors $\mathbf{B}^1$ and $\mathbf{C}^1$ can simply be obtained by inverting the matrix at the left side of Eq. (20) and all the subsequent coefficient vectors $\mathbf{B}^i$ and $\mathbf{C}^i$, in this example $i=2,3,\ldots,N$, can then be computed from them using Eq. (7). It is very obvious that the coefficient vectors and thus the electron wave function in the quantum channel depend on the wave vector $\mathbf{k}$ of the electron incident on the channel. We will therefore add on the wave function $\Psi^{i}(x,y)$ a subscript $\mathbf{k}$ to indicate this dependence.

For each incident wave $\mathbf{k}$, the electric current carried through the quantum channel by the wave function $\Psi_{\mathbf{k}}(x,y)$ can be expressed in terms of the expansion coefficients of the wave function in any one of the strip regions in the channel,

$$\begin{aligned}J(\varepsilon,\vartheta)&=\frac{ie\hbar}{2m^{*}}\int_{-w/2}^{w/2}dy\left[\Psi_{\mathbf{k}}^{*}(x,y)\frac{\partial}{\partial y}\Psi_{\mathbf{k}}(x,y)-\Psi_{\mathbf{k}}(x,y)\frac{\partial}{\partial y}\Psi_{\mathbf{k}}^{*}(x,y)\right]\\ &=-\frac{e\hbar}{2m^{*}}\sum_{n}\sum_{\alpha,\beta}d_{n\alpha}d_{n\beta}^{*}\{(k_{\alpha}+k_{\beta}^{*})[b_{\alpha}b_{\beta}^{*}e^{i(k_{\alpha}-k_{\beta}^{*})(x-x_{0})}-c_{\alpha}c_{\beta}^{*}e^{-i(k_{\alpha}-k_{\beta}^{*})(x-x_{0})}]\\ &\quad+(k_{\alpha}-k_{\beta}^{*})[b_{\alpha}c_{\beta}^{*}e^{i(k_{\alpha}+k_{\beta}^{*})(x-x_{0})}-c_{\alpha}b_{\beta}^{*}e^{-i(k_{\alpha}+k_{\beta}^{*})(x-x_{0})}]\} \ ,\end{aligned} \tag{22}$$

where ϑ specifies the incident direction of the electron wave in 2DEG and is defined as $\sin(\vartheta)=k_y/|k_x^2+k_y^2|^{1/2}$, $\varepsilon=\hbar^2(k_x^2+k_y^2)/2m^*$ is the energy of the incident electron. Here, the superscript i (the strip region index) has been dropped. Equation (22) can greatly be simplified if we evaluate the current using the expansion coefficients of the wave function $\Psi_{\mathbf{k}}(x,y)$ in a strip region in which $V_b^i(y)=0$. In this case, $d_{n\alpha}=\delta_{n\alpha}$ and the current is

$$J(\varepsilon,\vartheta)=-\frac{e\hbar}{m^{*}}\left[\sum_{n}^{(R)}k_{n}(b_{n}b_{n}^{*}-c_{n}c_{n}^{*})+\sum_{n}^{(I)}k_{n}(b_{n}c_{n}^{*}-C_{n}b_{n}^{*})\right] , \tag{23}$$

where (R) $[(I)]$ indicates that the sum is taken over those values of n for which k_n is real (imaginary).

At $T=0$, the conductance of the quantum channel is given by $G=|I/V|$, where V is a potential difference between the two 2DEG's, which causes a flow of electrons from left to right, and I is the sum of the contributions to the current from all the incident wave $\mathbf{k}$ on the channel from the left reservoir in the energy widow (E_F-eV,E_F) at the Fermi energy E_F. In the linear response regime, where V is assumed to be very small, the energy window is very narrow and the conductance of the quantum channel can then be written as

$$G=-\frac{4\pi em^{*}}{h^{2}}\int_{-\pi/2}^{\pi/2}d\vartheta\,J(E_{F},\vartheta) . \tag{24}$$

We note that the method presented in this section is formulated in a basis of infinite order and is exact. However, Eqs. (6) have to be solved numerically by truncating n and m at a high transverse level M. In the present calculations we let M be as large as it is necessary to obtain a desired convergence in the conductance and we seldom need to be beyond $M=7$. We further note that the method is also very general and has a great flexibility. The method can be easily used to treat the ballistic transport in the quantum confinements having very complicated structures in both the longitudinal and the transverse directions.

III. NUMERICAL RESULTS AND DISCUSSION

In this section, we will report on the results of the applications of our theoretical method to the quantum wire structures modulated with single and multiple double-

bend discontinuities. All our calculations have been performed with the assumption of an effective mass $m^*=0.067m_e$ which is appropriate to the $Al_xGa_{1-x}As/GaAs$ interface. In this work, we have chosen to plot the conductance G as a function of a dimensionless variable $\xi=(w/\pi\hbar)(2m^*E_F)^{1/2}$, where w is the width of the straight square-well channel delimited by hard walls and the E_F is the Fermi energy in the 2DEG's. It is very clear that ξ depends linearly on w and on $E_F^{1/2}$. From an experimental point of view one would like to vary the width of the quantum channel w by means of, e.g., an applied split-gate voltage. However, it is very convenient in theoretical calculations to vary the Fermi energy E_F while keeping w constant. In the present calculations, we have assumed $w=100$ nm. Thus ξ will depend on E_F only and will be called the renormalized Fermi energy.

We have first applied our theoretical method to the quantum channels with a double-bend discontinuity. We have idealized our channel structures by implanting two rectangular barriers of a finite height V_0 in the straight square-well channel of width w delimited by hard-wall boundaries. Figure 2 shows the calculated conductance G for the quantum channel with such a double-bend modulation of different barrier height V_0. The geometrical detail of the double-bend structure is shown in the inset of Fig. 2. At $V_0=0$, the considered structure is just the straight square-well channel with hard-wall boundaries. Figure 2(a) shows the calculated conductance for this case. The feature that the conductance is quantized in units of $2e^2/h$ is seen in this figure. The oscillations that appear at the edges of the quantized conductance

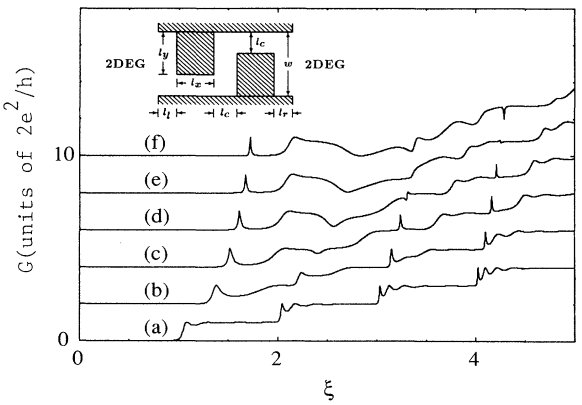

FIG. 2. Calculated conductance G as a function of renormalized Fermi energy $\xi=(w/\hbar\pi)(2m^*E_F)^{1/2}$ for the quantum channel with a double-bend modulation established by implanting two rectangular barriers of a finite height in a straight square-well channel of width w delimited by hard-wall boundaries. The geometrical detail of the double-bend structure is shown in the inset of this figure with $w=100$ nm, $l_x=50$ nm, $l_y=60$ nm, $l_l=l_r=30$ nm, and $l_c=w-l_y=40$ nm. The strength of the double-bend modulation is defined by the barrier height V_0. The curves in this figure show the conductance G calculated for different values of strength V_0 and have been offset vertically for clarity: (a) $V_0=0$, (b) $V_0=2\varepsilon_1$, (c) $V_0=4\varepsilon_1$, (d) $V_0=6\varepsilon_1$, (e) $V_0=8\varepsilon_1$, and (f) $V_0=10\varepsilon_1$.

plateaus are due to the formation of the longitudinal resonant states in the constriction.[7] In a weak modulation, i.e., in a small barrier potential V_0, this feature in the conductance of the straight square-well channel is seen to be only slightly disturbed. By comparing Fig. 2(b) to Fig. 2(a), one sees that at $V_0=\varepsilon_1$, where $\varepsilon_1=(\hbar^2/2m^*)(\pi/w)^2$ is the lowest transverse-mode energy of the straight square-well channel with the hard-wall boundaries, the step structure remains in the calculated conductance for high renormalized Fermi energy ξ. However, deviations in the conductance from the novel plateau structure clearly appear in the first few lowest plateaus. Especially, the first plateau has been suppressed overall except at the edge and the end of the plateau. At the edge of the plateau, a conductance peak can be identified. This peak becomes sharper as the strength V_0 of the modulations increases [see Figs. 2(c)–2(f)], and appears as a δ-function-like peak at $V_0=50\varepsilon_1$ [see Figs. 3(d) and 4(b)]. We have also examined the development of the peak as the length l_x of the two narrow straight parts of the double-bend structure increases. The results are shown in Fig. 3. It is seen that as l_x increases, the peak becomes narrower, whereas the height and position of the peak remain rather unchanged. This strongly indicates that the peak is associated with an electron state well localized in the junction part of the double-bend structure, i.e., the region in between the two rectangular barriers.

In recent works by Exner and Seba[13] and by Goldstone and Jaffe,[16] it was rather rigorously proved that in a curved quantum channel there exist at least one electron bound state or localized state at energy below the first transverse-mode energy (i.e., the bottom energy of the lowest subband). A more intuitive proof of the existence of such bound states in a sharp bend quantum channel can be found in Ref. 15. In these works the quantum channels have been assumed to be infinitely long. Our

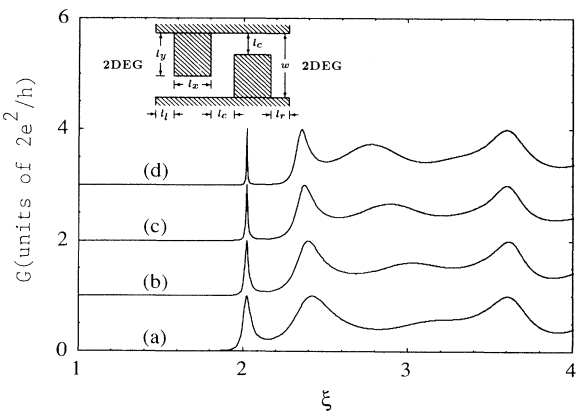

FIG. 3. Calculated conductance G as a function of renormalized Fermi energy $\xi=(w/\hbar\pi)(2m^*E_F)^{1/2}$ for the quantum channel with a double-bend modulation at a fixed strength $V_0=50\varepsilon_1$. The curves in this figure show the conductance G calculated for different values of l_x and have been offset vertically for clarity: (a) $l_x=20$ nm, (b) $l_x=30$ nm, (c) $l_x=40$ nm, and (d) $l_x=50$ nm. The geometrical detail of the double-bend structure is shown in the inset of this figure. All the unspecified parameters are the same as in Fig. 2.

above results have provided a numerical proof for the existence of localized state with energy below the first transverse-mode energy in a double-bend quantum channel. Since here we consider electron states in the quantum channels of finite length and being connected with the two 2DEG's, we prefer to call these localized states quasibound states. This is because the wave functions of these states spill over somehow onto the 2DEG regions. The sharp peak in the conductance as shown in Fig. 3(d) [also in Fig. 4(b)] corresponds to resonant tunneling via such a quasibound state. In addition to the sharp peak a broadened peak resonant with the bottom of the first plateau can also be seen in Fig. 3(d), indicating there exists another quasibound state at the edge of the first subband. We believe that when the barrier height V_0 approaches infinity this quasibound state should eventually be located at an energy well below the edge of the first subband.

In Fig. 4 we also display the calculated conductance in the quantum channel with the single double bend for different ratio l_c/w, where $l_c=w-l_y$ is the width of the doubly bent quantum channel formed by implanting two rectangular barriers in the straight square-well channel of width w (see the inset of the figure). In the calculations presented in this figure, the barrier height is fixed at $V_0=50\varepsilon_1$. We may note that at the limit case of $V_0\to\infty$, the first transverse-mode energy, or the threshold of the first conductance plateau, of the doubly bent quantum channel is given by $\hbar^2(\pi/l_c)^2/(2m^*)=\varepsilon_1/(l_c/w)^2$. Figures 4(a) and 4(b) show the calculated conductance for the doubly bent quantum channels with $l_c/w=0.3$ and 0.4, respectively, in which electrons are forced through a double-bend discontinuity when the Fermi energy E_F is lower than the barrier height V_0. In these figures, particularly in Fig. 4(a), the two peaks corresponding to resonant tunneling via quasibound states below the threshold of the first conductance plateau of the doubly bent quantum channel are seen. The peak at an energy farther below the threshold of the first plateau is rather sharp, while the peak at an energy closer to the threshold is quickly broadened as the value of l_c/w is increased. The calculated conductance for the doubly bent quantum channel with $l_c/w=0.5$ is shown in Fig. 4(c). The value, 0.5, is the allowed maximum value of l_c/w for the maintenance of a complete double-bend discontinuity in our quantum system. Here we can see that the peak farther below the threshold of the first conductance plateau remains sharp, while the other peak just appears as a very weak bump at the threshold of the plateau. Figures 4(d) and 4(e) display the calculated conductance for the channel with $l_c/w=0.6$ and 0.7, respectively, in which a straight open strip along the transport x direction is provided for electron motion. Only one conductance peak at an energy below the threshold of the first plateau is seen in Figs. 4(d) and 4(e), indicating that there can only be one quasibound state at energy below the first transverse mode in these lateral structures.

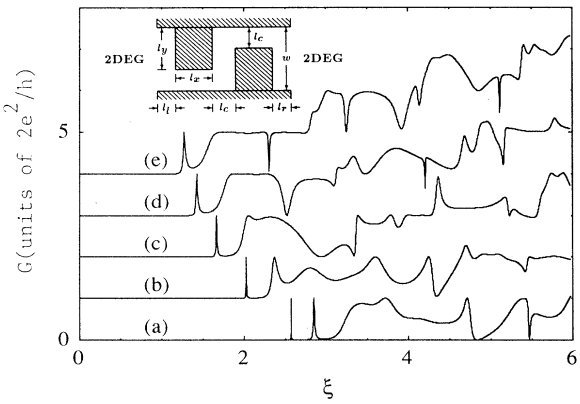

FIG. 4. Calculated conductance G as a function of renormalized Fermi-energy $\xi=(w/\hbar\pi)(2m^*E_F)^{1/2}$ for the quantum channel with a double-bend modulation at a fixed strength $V_0=50\varepsilon_1$. The curves in this figure show the conductance G calculated for different values of l_c, which has been set to $w-l_y$ and defines exactly the width of the doubly bent channel at $V_0\to\infty$: (a) $l_c=30$ nm, (b) $l_c=40$ nm, (c) $l_c=50$ nm, (d) $l_c=60$ nm, and (e) $l_c=70$ nm. The geometrical detail of the double-bend structure is shown in the inset of this figure. All the unspecified parameters are the same as in Fig. 2. The curves have been offset vertically for clarity.

In a recent experiment,[12] interference phenomena due to a double bend in a quantum channel were observed. The lateral structure of the quantum channel studied in this work may be considered to be analogous to our model structures with $l_c/w<0.5$ [e.g., the structures used for calculations of the conductance presented in Figs. 4(a) and 4(b)]. The authors of this work observed also two sharp conductance peaks below the threshold of the first conductance plateau.[12] They argued that the two peaks originate from resonant tunneling through impurity states in the quantum channel. However, our calculations strongly suggest that the two peaks observed in this experiment may well be due to the resonant tunneling through quasibound states. Thus we call for experimental reexaminations on this issue. We believe that the two conductance peaks should appear at low temperature as a fundamental phenomenon due to the presence of quasibound states below the first transverse mode in such a quantum confinement.

A theoretical investigation on electron transport through a doubly bent quantum channel has also been carried out recently by Weisshaar *et al.*[17] In this work only the double bend itself is basically included in the calculations while assuming that the two straight channels that are connected together through the double-bend junction are infinitely long. The authors of this study only reported the calculations of the total transmission probability from individual modes, not the conductance, for the doubly bent quantum channel. Thus a direct comparison of our calculations with theirs cannot be done. However, we wish to note that due to their use of the assumption that the channels which are doubly bent are infinitely long, these authors were unable to find the transmission peaks corresponding to resonant tunneling via bound states below the first transverse mode of the channel. This is because these bound states are entirely confined to the quantum channel and cannot be coupled to incoming and outgoing waves at infinity. Thus we wish to stress that in order to probe such bound states in

a quantum channel via electron transmissions, it is essential to set the quantum channel to be of finite length and consider electron states in much wider outside regions that are connected with the channel.

In Fig. 4 we can also see that when going from Fig. 4(e) down to Fig. 4(a), both the threshold of the first conductance plateau and the sharp conductance peaks due to resonant tunneling via the quasibound states below the threshold are shifted towards high renormalized Fermi energy ξ. This is consistent with the fact that in this order the doubly bent quantum channel tends to be narrow. In addition to the appearance of the quasibound states, the conductance plateau structure is seen to be strongly distorted. Many dips appear in the conductance plateaus. This is so even in the case that a straight open strip for electron motion is actually present in the channel [see Figs. 4(d) and 4(e)]. These dips, often called antiresonances, originate from interferences of electron waves due to the double-bend discontinuity in the quantum channels.

A multiple double-bend discontinuity in a narrow quantum channel can be obtained by introducing more than two rectangular barriers in the channel. Two such quantum structures are shown in the insets of Figs. 5(a) and 5(b). When the height of the barriers in the quantum channel is set to infinity, these two structures may be called double and triple doubly bent quantum wires, respectively. In the cases that the barrier height V_0 is finite, the structures can still be considered as the double and triple doubly bent quantum wires for electron transport at Fermi energies far enough below the height V_0. In the calculations for the quantum channels with these two multiple double-bend discontinuities we have assumed $V_0=4\varepsilon_1$, since here we are mainly interested in the conductance peaks corresponding to resonant tunneling via quasibound states below the first transverse mode of the quantum channel. We display in Figs. 5(a) and 5(b) the calculated conductance for these quantum structures with this barrier height. The calculated conductance for the corresponding quantum channel with the single double-bend discontinuity may be found in Fig. 2(c). At energies below the threshold of the first conductance plateau, we find one conductance peak in the quantum channel with the single double-bend discontinuity [see Fig. 2(c)], two peaks in the channel with the double double-bend discontinuity [Fig. 5(a)], and three peaks in the channel with triple double-bend discontinuity [Fig. 5(b)]. This finding is also expected to be correct for these multiple doubly bent quantum channels with the barriers of infinite height. Thus we may conclude that a conductance peak below the threshold of the first conductance plateau in the quantum wire with a single double bend is split into N peaks in the quantum wire with N sequential and aligned double bends. This result clearly indicates a formation of N-fold splitting quasibound states in the system due to the coupling between the quasibound states localized in different double-bend junctions. We like to note that for the geometry of the double-bend junctions we have investigated, there can be two quasibound states at energies below the first transverse mode in each junction when the height of the barriers defining the junction is infinite [see Figs. 3(d) and 4(b) for an approximate case]. Therefore, as V_0 approaches infinity, we should find two sets of N-fold splitting quasibound states below the the first transverse mode in the quantum wire with N sequential and aligned double bends, provided that the couplings between quasibound states in adjacent double-bend junctions are not too strong. As a consequence, two sets of N-fold splitting resonant peaks in the conductance should appear at energies below the threshold of the first conductance plateau in the N-fold double-bend quantum wire in this case. Finally, we mention that Figs. 5(a) and 5(b) also show that the dips in the conductance become deeper and the bottoms of the dips become wider as the number of double bends in the quantum wire is increased. This may suggest that experimental observation on the effects of interferences in the ballistic regime become easier in the quantum wire with a larger number of double-bend junctions.

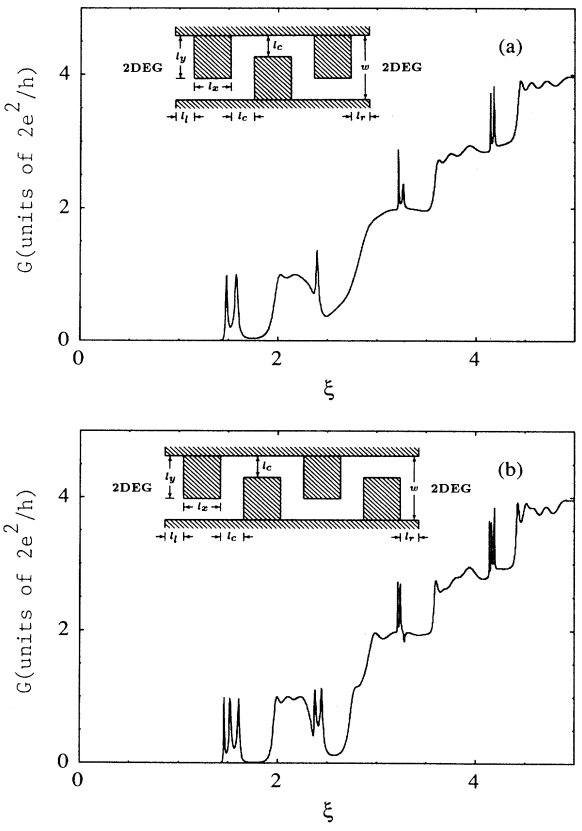

FIG. 5. Calculated conductance G as a function of renormalized Fermi energy $\xi=(w/\hbar\pi)(2m^*E_F)^{1/2}$ for the quantum channel with (a) a double and (b) a triple double-bend modulation at a fixed strength $V_0=4\varepsilon_1$. The geometrical details of the two multiple double-bend structures are shown in the insets of the two figures. All the unspecified parameters are the same as in Fig. 2.

IV. SUMMARY AND CONCLUDING REMARKS

In this paper we have reported on exact quantum-mechanical calculations of electron transport in narrow quantum channels with single and multiple double-bend

discontinuities. In order to model the transport in the ballistic regime and, particularly, to probe quasibound states by means of electron transmission, we have assumed that the channels are of finite length and are connected with 2DEG's, which acts as source and drain when a potential difference is applied. A transfer-matrix method has been formulated and used in the calculations. We have based all our matrices throughout the quantum channel on one common basis. Thus the method has a great flexibility, i.e., it can be easily used to treat electron transport in the quantum channels having very complicated structures in both the longitudinal and the transverse directions.

The method has first been used to investigate the electron transport in the narrow quantum channel with a single double-bend modulation of different strength V_0. We have shown that for a large enough modulation strength V_0, at least one conductance peak corresponding to resonant tunneling via quasibound state of the double-bend structure can appear at an energy below the threshold of the first conductance plateau. We have found that the number of resonant conductance peaks that appear at energies below the threshold of the first conductance plateau depends on the ratio l_c/w (see, for example, the schematic illustration in the inset of Fig. 4 for l_c and w). We have shown that, at a strong doubly bent modulation, two conductance peaks at energies below the threshold of the first conductance plateau can appear when the ratio l_c/w is smaller than 0.5, whereas only one peak at an energy below the threshold of the first plateau can appear when the ratio l_c/w is larger than 0.5. Thus our calculations have provided a numerical proof of the existence of the quasibound states below the first transverse-mode energy in a double bent quantum channel. Based on these results we have proposed that the two conductance peaks observed by Wu *et al.*[12] at gate voltage below the threshold of the first conductance plateau may well be interpreted in terms of resonant tunneling via quasibound states. We have stressed that in order to find theoretically such quasibound states via electron transmissions, it is crucial to set the quantum channel to be of finite length and consider electron states in much wider outside regions connected with the channel. We have further applied our theoretical method to the quantum channels with multiple double-bend discontinuities. We have shown that each conductance peak at the energy below the threshold of the first conductance plateau is split into N peaks in the quantum channel with N sequential and aligned double bends and that the dips in the conductance become deeper and the bottoms of the dips become wider as the number of double bends in the quantum channel increases.

The two conductance peaks corresponding to the resonant tunneling via quasibound states at energies below the first transverse mode in a doubly bent quantum channel were also found in the calculations by Wu, Sprung, and Martorell[18] with the use of the single-mode approximation leading to a description of the channel simply by a one-dimensional double square well.

ACKNOWLEDGMENTS

The author is grateful to L. Hedin at the Department of Theoretical Physics, University of Lund for his support of this work in part and to K.-F. Berggren, Linköping University, for many stimulating discussions. The author wishes to thank P. Omling and L. Samuelson, University of Lund, for encouragement, support, and conversations. The author also acknowledges many useful discussions with Zhen-Li Ji, Linköping University. The calculations have been done in part on the computing facilities of the Solid State Theory Group, Department of Theoretical Physics, University of Lund. This work has been supported by the Swedish Natural Science Research Council and the Swedish Engineering Research Council.

*Also at Department of Theoretical Physics, University of Lund, Sölvegatan 14 A, S-223 62 Lund, Sweden.

[1]See, e.g., M. L. Roukes *et al.*, in *Science and Engineering of 1- and 0-Dimensional Semiconductors,* edited by S. P. Beaumont and C. M. Sotomayor-Torres (Plenum, New York, 1989), for a survey of microfabrication techniques of nanostructures.

[2]C. W. Beenakker and H. van Houten, in *Solid State Physics: Advances in Research and Applications,* edited by H. Ehrenreich and D. Turnbull (Academic, New York, 1991), Vol. 44, p. 1.

[3]B. J. van Wees, H. van Houten, C. W. J. Beenakker, J. G. Williamson, L. P. Kouwenhoven, D. van der Marel, and C. T. Foxon, Phys. Rev. Lett. **60**, 848 (1988).

[4]D. A. Wharam, T. J. Thornton, R. Newbury, M. Pepper, and H. Ahmed, J. Phys. C **21**, L209 (1988).

[5]L. P. Kouwenhoven, F. W. J. Hekking, B. J. van Wees, and C. J. P. M. Harmans, Phys. Rev. Lett. **65**, 361 (1990).

[6]K.-F. Berggren and Zhen-li, Ji, Superlatt. Microstruct. **8**, 59 (1990); Phys. Rev. B **43**, 4760 (1991).

[7]G. Kirczenow, Solid State Commun. **68**, 715 (1988); J. Phys. Condens. Matter **1**, 305 (1989); Phys. Rev. B **39**, 10 452 (1989).

[8]R. L. Schult, D. G. Ravenhall, and H. W. Wyld, Phys. Rev. B **39**, 5476 (1989).

[9]J. A. Brunn, Phys. Rev. B **43**, 12 082 (1991).

[10]F. M. de Aguiar and D. A. Wharam, Phys. Rev. B **43**, 9984 (1991).

[11]Hua Wu, D. W. L. Sprung, J. Martorell, and S. Klarsfeld, Phys. Rev. B **44**, 6351 (1991).

[12]J. C. Wu, M. N. Wybourne, W. Yindeepol, A. Weisshaar, and S. M. Goodnick, Appl. Phys. Lett. **59**, 102 (1991).

[13]P. Exner and P. Seba, J. Math. Phys. **33**, 2574 (1989).

[14]F. Sols and M. Macucci, Phys. Rev. B **41**, 11 887 (1990).

[15]Y. Avishai, D. Bessis, B. G. Giraud, and G. Mantica, Phys. Rev. B **44**, 8028 (1991).

[16]J. Goldstone and R. L. Jaffe, Phys. Rev. B **45**, 14 100 (1992).

[17]A. Weisshaar, J. Lary, S. M. Goodnick, and V. K. Tripathi, Appl. Phys. Lett. **55**, 2114 (1989).

[18]Hua Wu, D. W. L. Sprung, and J. Martorell, Phys. Rev. B **45**, 11 960 (1992).